The role of attractive many-body interaction in the gas–liquid transition of mercury

2007 J. Phys.: Condens. Matter 19 072102

(http://iopscience.iop.org/0953-8984/19/7/072102)

IOP FTC

IOP PUBLISHING JOURNAL OF PHYSICS: CONDENSED MATTER

J. Phys.: Condens. Matter **19** (2007) 072102 (7pp) doi:10.1088/0953-8984/19/7/072102

FAST TRACK COMMUNICATION

The role of attractive many-body interaction in the gas–liquid transition of mercury

Hikaru Kitamura

Department of Physics, Kyoto University, Sakyo-ku, Kyoto 606-8502, Japan

Received 1 December 2006
Published 2 February 2007
Online at stacks.iop.org/JPhysCM/19/072102

Abstract

The equation of state for expanded fluid mercury based on the variational associating fluid theory is developed to elucidate the mechanisms of the gas–liquid transition in terms of microscopic interatomic interaction. The theory describes the interaction of an atom with its neighbouring atoms through an effective many-body potential, which is constructed through quantum-chemical calculations of cohesive energies for selected geometries of clusters and bulk crystals. The overall feature of the observed gas–liquid coexistence curve is reproduced accurately without introducing phenomenological adjustable parameters. It is shown that the local aggregation of atoms produces a strong cohesive force due to a change in the local electronic states, which plays a crucial role in the gas–liquid transition. The predicted phase behaviour is consistent with the picture of inhomogeneous expansion, in which the average coordination number is nearly proportional to the average density along the coexistence curve.

It is a fundamental and challenging issue of condensed matter physics to predict the macroscopic phase behaviour of an elementary substance with first-principles theories [1]. For a simple fluid, in which the constituent atoms mutually interact via pairwise-additive binary forces, thermodynamic quantities and gas–liquid coexistence curves can be calculated either by analytic theories or by simulations [2]. Mercury, one of the most prototypical materials of all the fluid metals, may be regarded as a *non-simple* fluid in the sense that its interatomic interaction depends strongly on thermodynamic states: metallic bonding in the liquid phase differs considerably from the van der Waals bonding in the gas phase [3]. Moreover, due to the density fluctuation inherent in fluids, the strength of interatomic interaction may be influenced sensitively by a change in the local atomic environment, such as temporary clustering (i.e., *association*) [4].

In this communication, we report on a new equation of state for expanded fluid mercury based on the variational theory of statistical physics, taking additional account of the association effect and quantum chemical modelling of microscopic many-body interaction. To the author's

knowledge, this is the first theory to *predict* the gas–liquid coexistence curve of elementary mercury from room temperature to the critical point by using *ab initio* interatomic potentials as input. Moreover, the formalism is quite general and would be applicable to other liquids after suitable modifications.

An isolated Hg atom has the closed-shell $6s^2\ {}^1S_0$ electronic configuration in the ground state. The potential energy curve, $V_{\rm dimer}(r)$, of a Hg_2 dimer in the ground state was computed by Schwerdtfeger *et al* [5] based on spin–orbit corrected scalar relativistic coupled cluster calculations. The analytic formula for $V_{\rm dimer}(r)$ in their s-cc-ULB + SO scheme is available in table 1 of [5]. In terms of $V_{\rm dimer}(r)$, the potential energy function of a fluid consisting of N mercury atoms is written generally as

$$V(\mathbf{r}_1, \ldots, \mathbf{r}_N) = \frac{1}{2} \sum_{\substack{i,j=1 \\ i \neq j}}^{N} V_{\rm dimer}(|\mathbf{r}_i - \mathbf{r}_j|) + V_{\rm mb}(\mathbf{r}_1, \ldots, \mathbf{r}_N) \tag{1}$$

where $\mathbf{r}_i$ denotes the positional vector of the ith nucleus. Because the binding energy of Hg_2 amounts to 0.043 eV [5], and this value is far smaller than observed gas–liquid critical temperature, $T_{\rm c}({\rm exp}) = 1751\ {\rm K} = 0.151$ eV, the bulk of the cohesive force responsible for the gas–liquid transition should arise from the many-body potential, $V_{\rm mb}$.

The basic idea of this work is to evaluate $V_{\rm mb}$ for particular geometries of clusters and crystalline solids, and to express $V_{\rm mb}/N$ as a function of two relevant parameters: z (mean coordination number) and $r_{\rm nn}$ (nearest-neighbour distance). For this purpose, we have carried out quantum-chemical diatomics-in-molecules calculations [6] of $V_{\rm mb}(z, r_{\rm nn})/N$ for small Hg_N clusters with the following ground-state geometries: equilateral triangle (D_{3h}) for $N = 3$, tetrahedron (T_d) for $N = 4$, trigonal bipyramid (D_{3h}) for $N = 5$, and pentagonal bipyramid (D_{5h}) for $N = 7$. These geometries may be characterized by mean coordination numbers of $z = 2$, 3, 3.60, and 4.29, respectively. Here, we have assumed breathing motions so that the value of $r_{\rm nn}$ for all the bonds within a cluster has been changed simultaneously in the range $5.3 \leqslant r_{\rm nn}/a_{\rm B} \leqslant 6.5$, with $a_{\rm B}$ denoting the Bohr radius. In this range, mercury clusters remain nonmetallic, with a finite energy gap between the ground and first-excited energy levels [6].

We have likewise evaluated $V_{\rm mb}(z, r_{\rm nn})/N$ for face-centred cubic (fcc; $z = 12$) and body-centred cubic (bcc; $z = 8$) structures of the bulk solids, which may be treated as divalent metals [3]. We have followed the modified pseudopotential approach by Chekmarev *et al* [7]: the Ashcroft empty-core pseudopotential has been used for the bare electron–ion interaction, with a core radius of $R_{\rm c} = 0.915a_{\rm B}$. Electron–electron correlation has been treated with the local-field correction by Ichimaru and Utsumi [8]. The resultant density-dependent ion–ion interaction has been modified by adding the Born–Mayer repulsive potential, as explained in [7]. An empirical correction to the structure-independent energy [7] has also been included as a function of the conduction electron density so as to reproduce the experimental cohesive energy of 0.67 eV/atom at $z = 12$.

Numerical values of $V_{\rm mb}(z, r_{\rm nn})/N$ so computed are displayed in figure 1. We find that the many-body interaction is attractive ($V_{\rm mb} < 0$) and its magnitude increases as $r_{\rm nn}$ decreases and/or z increases. This feature can be interpreted as the increasing admixture of the excited p state onto the ground s state in the electronic wavefunctions when more atoms come closer to each other [6]. The magnitude of $V_{\rm mb}(z, r_{\rm nn})/N$ is especially large for $z > 8$, reflecting a considerable deviation of the short-range interaction in the metallic phase from that in the isolated dimer.

We have no convincing theoretical data for $V_{\rm mb}(z, r_{\rm nn})$ in the intermediate-z range where the metal–nonmetal (M–NM) transition [3, 9] takes place. Therefore, we have linearly interpolated the data at $z = 4.29$ and 8 as shown by the solid curves in figure 1. Though

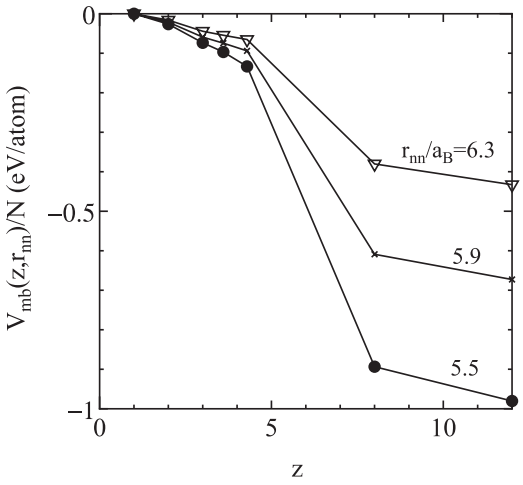

Figure 1. Many-body potential per atom. Dots, crosses, and triangles refer to computed data; the solid lines depict their interpolations.

this is a crude treatment of the M–NM transition, we remark that the experimental cohesive energies of Hg_N clusters by Haberland *et al* [9] exhibit similar crossover from nonmetallic to metallic behaviour in the range $N \approx 15$–100, which may correspond to $z \approx 7$–9 for icosahedral geometries or $z \approx 5$–8 for tetrahedral geometries [10]. It should be noted that their experiment may detect clusters whose bond lengths are close to the equilibrium values; the corresponding data for smaller or larger bond lengths are not exactly known.

For given atomic number density n and temperature T, the Helmholtz free energy F is formulated with the soft-sphere variational theory proposed by Ross [11]. We adopt the inverse sixth-power potential as a reference [12], with the recognition that the short-range repulsive part of $V_{\rm dimer}(r)$ is approximately proportional to $1/r^{6.2}$ [13]. Thus, $f \equiv F/Nk_{\rm B}T$ may be expressed as

$$f(n,T,\sigma) \approx f_{\rm id} - s_{\rm HS}^{\rm ex} + \frac{n}{2k_{\rm B}T}\int_{\sigma}^{\infty} {\rm d}r 4\pi r^2 V_{\rm dimer}(r) g_{\rm HS}(r) + \left\langle \frac{V_{\rm mb}(z,r_{\rm nn})}{Nk_{\rm B}T} \right\rangle_{\rm HS} + f_6. \qquad (2)$$

Here, $f_{\rm id} = \ln(\lambda^3 n) - 1$ represents the ideal-gas free energy with $\lambda = (2\pi\hbar^2/Mk_{\rm B}T)^{1/2}$, and $M = 3.331\times10^{-22}$ g is the mass of a Hg atom. The quantities with subscript 'HS' are evaluated for the hard-sphere fluid with core diameter σ. The quantity $s_{\rm HS}^{\rm ex} = -\eta(4-3\eta)/(1-\eta)^2$ denotes the excess entropy in the Carnahan–Stirling approximation [2], with $\eta = \pi n\sigma^3/6$ being the packing fraction. The last term, $f_6 = -0.932\,71\eta - 0.495\,05\eta^2 - 2.129\,24\eta^3 + 0.500\,30\eta^4$, represents the soft-sphere correction obtained by Young and Rogers [12]. The radial distribution function $g_{\rm HS}(r)$ for the hard-sphere fluid is available in parameterized form in Trokhymchuk *et al* [14].

In fluids, the coordination number z of an arbitrarily chosen atom may be defined as the number of nearest-neighbour atoms contained within a sphere of certain volume v ($= 4\pi r_{\rm max}^3/3$) encompassing that atom. In light of the observation in figure 1, we expect that an atom with larger z and/or smaller $r_{\rm nn}$ may feel stronger attractive force. Such a many-body effect is described by the term $\langle\cdots\rangle_{\rm HS}$ in equation (2), which we evaluate as

$$\left\langle \frac{V_{\rm mb}(z,r_{\rm nn})}{Nk_{\rm B}T} \right\rangle_{\rm HS} = \sum_{z=1}^{z_{\rm max}} p_{\rm HS}(z) \frac{\int_{\sigma}^{r_{\rm max}} {\rm d}r_{\rm nn} H_{\rm HS}(r_{\rm nn}) \frac{V_{\rm mb}(z,r_{\rm nn})}{Nk_{\rm B}T}}{\int_{\sigma}^{r_{\rm max}} {\rm d}r_{\rm nn} H_{\rm HS}(r_{\rm nn})}. \qquad (3)$$

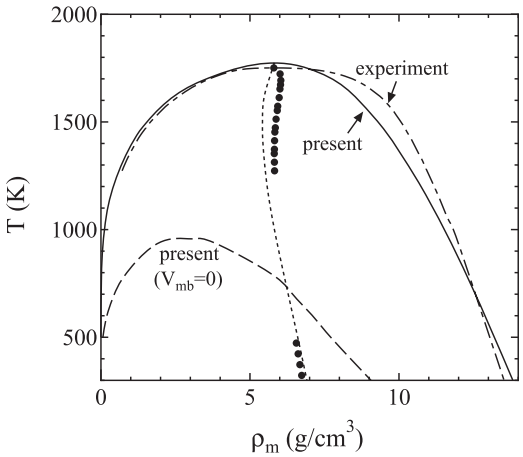

Figure 2. Gas–liquid coexistence curve on the mass density–temperature plane. The solid curve represents the full result; the dashed curve is the corresponding result with $V_{\rm mb} = 0$; the dash–dotted curve is experimental data [3, 16]. The mean density $\rho_{\rm d}$ in the present theory is plotted by the dotted curve; the corresponding experimental data [3, 16] are shown by the dots.

Here, $p_{\rm HS}(z)$ is the distribution function of z in the hard-sphere fluid. Within the excluded-volume approximation [4], we have $p_{\rm HS}(z) = [p_{\rm HS}(0)/z!](n\upsilon-\eta)(n\upsilon-2\eta)\cdots(n\upsilon-z\eta)/(1-\eta)^z$ for $1 \leqslant z \leqslant z_{\rm max}$; $p_{\rm HS}(0)$ is determined from the normalization, $\sum_{z=0}^{z_{\rm max}} p_{\rm HS}(z) = 1$. In this work, we take the maximum value of z as $z_{\rm max} = 12$ (corresponding to the fcc lattice), and υ is chosen as $\upsilon = (z_{\rm max}+1)\pi\sigma^3/6$, leading to $r_{\rm max} = (z_{\rm max}+1)^{1/3}\sigma/2 = 1.176\sigma$. In this case, it can be proven that the average coordination number, $\langle z\rangle \equiv \sum_{z=0}^{z_{\rm max}} z p_{\rm HS}(z)$, is proportional to the packing fraction as $\langle z\rangle = z_{\rm max}\eta$.

The distribution function $H_{\rm HS}(r_{\rm nn})$ represents the probability of finding a nearest-neighbour particle at distance $r_{\rm nn}$ from the reference particle. The properties of this function were discussed in detail by Torquato [15]. We adopt the analytic expression given by equation (43) of [15]. We note that $H_{\rm HS}(r_{\rm nn})$ is a decreasing function of $r_{\rm nn}$ with a peak at $r_{\rm nn} = \sigma$; the peak becomes sharper as η increases.

For given n and T, the total free energy $f(n, T, \sigma)$ is minimized with respect to the variational parameter, σ. The pressure P and Gibbs free energy G are then calculated as $p \equiv P/nk_{\rm B}T = n(\partial f/\partial n)_T$ and $G/Nk_{\rm B}T = f + p$. The gas–liquid transition densities, $n_{\rm gas}$ and $n_{\rm liq}$, are obtained in accordance with the conditions of two-phase equilibrium, $P(n_{\rm gas}, T) = P(n_{\rm liq}, T)$ and $G(n_{\rm gas}, T) = G(n_{\rm liq}, T)$. The gas–liquid coexistence curves so obtained are displayed in figure 2 ($\rho_{\rm m}$–T diagram; $\rho_{\rm m} \equiv Mn$) and in figure 3 (T–P diagram). It can be seen that the theoretical coexistence curves reproduce the experimental data [3, 16] reasonably well. The critical density, temperature, and pressure are predicted to be $\rho_{\rm c} = 5.82$ g cm^{-3}, $T_{\rm c} = 1774$ K, and $P_{\rm c} = 1.97$ kbar, respectively, which are in good agreement with the corresponding experimental values [3], $\rho_{\rm c}({\rm exp}) = 5.8$ g cm^{-3}, $T_{\rm c}({\rm exp}) = 1751$ K, and $P_{\rm c}({\rm exp}) = 1.67$ kbar. The liquid density at the melting point ($T = 234$ K, $P = 1$ bar) turns out to be 14.02 g cm^{-3}, which is comparable to the experimental value, 13.65 g cm^{-3}.

For comparison, we have repeated the same calculation by setting $V_{\rm mb} = 0$ in equation (2). The resultant coexistence curves, shown by dashed curves in figures 2 and 3, clearly indicate that the attractive interaction associated with $V_{\rm dimer}(r)$ is too weak to account for the observed gas–liquid transition.

In figure 2, we also plot the average of the gas and liquid densities, $\rho_{\rm d} \equiv M(n_{\rm gas}+n_{\rm liq})/2$. According to the experimental data [3, 16], starting from sufficiently low temperature, $\rho_{\rm av}$

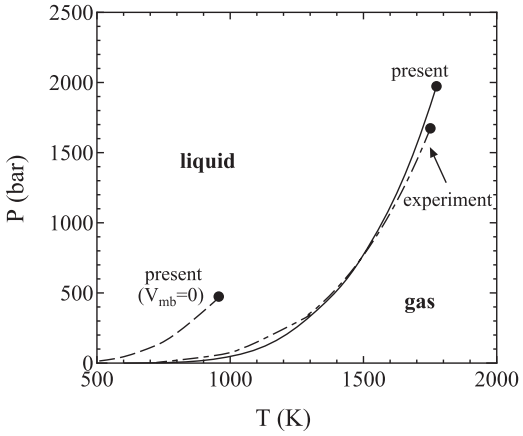

Figure 3. Same as figure 2 but on the temperature–pressure plane. The dots depict the critical points.

first decreases as T increases, and then it starts to increase when T exceeds about 1300 K. It is remarkable that such skewing behaviour is qualitatively reproduced by the present theory above 1500 K. The modified two-state van der Waals model of Ross and Hensel [17] indicated that the change in the slope of ρ_d is interrelated with the M–NM transition in the liquid phase. Experimentally, ρ_d shifts again to lower density in the very vicinity of the critical point, which cannot be reproduced by our equation of state.

Because the present theory contains structural information for the reference hard-sphere fluid, it is instructive to list the values of the optimized core diameter in the liquid phase along the coexistence curve: $\sigma/a_B = 5.59$ ($\rho_m = 5.8$ g cm^{-3}, $T = 1774$ K), 5.58 (11.5 g cm^{-3}, 1000 K), and 5.67 (13.8 g cm^{-3}, 300 K). Thus, σ remains virtually constant in the density range, $\rho_m = 5.8$–11.5 g cm^{-3}, in spite of considerable decrease of T. In this density range, we find the proportionality relation, $\langle z \rangle \approx 0.49\rho_m$ (g cm^{-3}), which embodies the picture of inhomogeneous expansion [18].

In figure 4, the distribution function $p_{HS}(z)$ is illustrated and compared with the data of reverse Monte Carlo (RMC) simulation by Arai and McGreevy [19] deduced from the measured structure factors of mercury. At $\rho_m = 6.8$ g cm^{-3}, $p_{HS}(z)$ is virtually confined within the nonmetallic regime, with a peak at $z = 3$. At the normal liquid density at 293 K, the peak is located at $z = 7$, where strong cohesive force due to metallic bonding is expected, as we see in figure 1. The RMC distribution functions systematically shift to the low-z side, probably because r_{max} was fixed at a relatively small value of $6.05a_B$ [19]; we adopt $r_{max} = 1.176\sigma \approx 6.67a_B$ in this work.

The influence of many-body interaction on the coexistence curve was studied by several investigators from different viewpoints. Raabe and Sadus [20] replaced V_{mb} by an effective potential of the form $C(T)/r^9$, where $C(T)$ was determined to match the experimental liquid density below 1073 K. We have not introduced such phenomenological T- or n-dependent factors in the interatomic potentials. Redmer and collaborators [21] treated fluid mercury as a partially ionized non-ideal plasma composed of ions, conduction electrons and neutral atoms. The shape of their coexistence curve on the ρ_m–T plane is somewhat too sharp; the same tendency was found in our previous calculation as well [22]. This would imply that the delocalized electrons do not extend uniformly over the entire space but rather that the local electronic states are governed by local density fluctuation, as pointed out by Chacón *et al* [23]

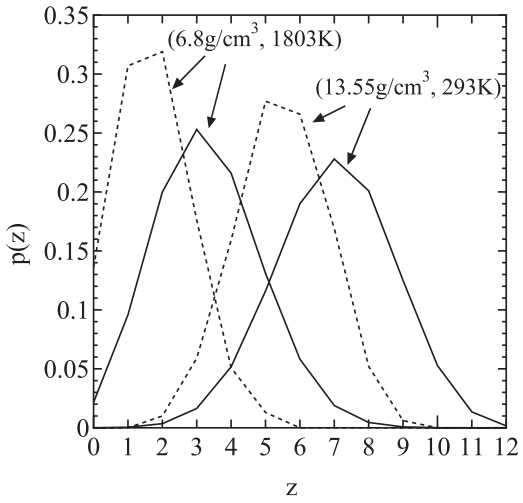

Figure 4. Distributions of coordination number at $(\rho_m, T) = (13.55\ \mathrm{g\,cm^{-3}}, 293\ \mathrm{K})$, $(6.8\ \mathrm{g\,cm^{-3}}, 1803\ \mathrm{K})$. The solid curves depict $p_{HS}(z)$; the dotted curves, the reverse Monte Carlo (RMC) data by Arai and McGreevy [19].

in their lattice gas theory of fluid alkali metals. A salient feature of the present theory is that the effect of density fluctuation is included through $p_{HS}(z)$ *without* assuming a hypothetical lattice.

The present formalism is closely related to the earlier theoretical model by Rosenfeld [24]. He utilized zero-temperature equations of state for solids as the *only* input information, and successfully explained the experimental critical points for rare gases and alkali metals, but not for mercury. His theory assumed that the interaction energy of an atom in the fluid is proportional to the local coordination number, and hence the former was evaluated by extrapolating the solid-state data at $z = 12$ towards the small-z regime [24, 25]. We claim that such an extrapolation is not valid for mercury, because the interaction energies in the metallic and nonmetallic regimes behave in quite different manners, as we see in figure 1. We also remark that, in the low-density gas phase with $\langle z \rangle \approx 0$, the interaction part of equation (2) is dominated by the accurate diatomic potential $V_{dimer}(r)$, which is absent in the theory of Rosenfeld [24].

In conclusion, we have developed a variational equation of state for expanded fluid mercury by taking into account the cooperative interatomic interaction associated with local density fluctuation. Our equation of state can successfully reproduce the observed gas–liquid coexistence curve. As the density increases, the atomic coordination number increases, giving rise to a change in the local electronic states and the creation of strong attractive many-body forces among the atoms. Such associative interaction plays a dominant role in the gas–liquid transition of mercury.

The author thanks Dr F Hensel, Dr R M More, Dr R Redmer, Dr M Yao, and Dr H Yoneda for pertinent discussions. This work was supported in part through a Grant-in-Aid for Scientific Research provided by the Japanese Ministry of Education, Science, Sports and Culture.

References

[1] Young D A 1991 *Phase Diagrams of the Elements* (Berkeley, CA: University of California Press)
[2] Hansen J-P and McDonald I R 1990 *Theory of Simple Liquids* 2nd edn (London: Academic)

[3] Hensel F and Warren W W Jr 1999 *Fluid Metals* (Princeton, NJ: Princeton University Press) chapter 4
[4] Bhatt R N and Rice T M 1979 *Phys. Rev.* B **20** 466
[5] Schwerdtfeger P, Wesendrup R, Moyano G E, Sadlej A J, Grief J and Hensel F 2001 *J. Chem. Phys.* **115** 7401
[6] Kitamura H 2006 *Chem. Phys. Lett.* **425** 205
[7] Chekmarev D S, Zhao M and Rice S A 1999 *Phys. Rev.* E **59** 479
[8] Ichimaru S and Utsumi K 1981 *Phys. Rev.* B **24** 7385
[9] Haberland H, Kornmeier H, Langosch H, Oschwald M and Tanner G 1990 *J. Chem. Soc. Faraday Trans.* **86** 2473
[10] Fritsche H-G and Benfield R E 1993 *Z. Phys.* D **26** (Suppl.) S15
[11] Ross M 1979 *J. Chem. Phys.* **71** 1567
[12] Young D A and Rogers F J 1984 *J. Chem. Phys.* **81** 2789
[13] Koperski J 2002 *Phys. Rep.* **369** 177
[14] Trokhymchuk A, Nezbeda I, Jirsák J and Henderson D 2005 *J. Chem. Phys.* **123** 024501
[15] Torquato S 1995 *Phys. Rev.* E **51** 3170
[16] Mehdipour N and Boushehri A 1997 *Int. J. Thermophys.* **18** 1329
[17] Ross M and Hensel F 1996 *J. Phys.: Condens. Matter* **8** 1909
[18] Tamura K and Inui M 2001 *J. Phys.: Condens. Matter* **13** R337
[19] Arai T and McGreevy R L 1998 *J. Phys.: Condens. Matter* **10** 9221
[20] Raabe G and Sadus R J 2003 *J. Chem. Phys.* **119** 6691
[21] Redmer R 1997 *Phys. Rep.* **282** 35
[22] Kitamura H 2003 *J. Phys.: Condens. Matter* **15** 6427
[23] Chacón E, Hernandez J P and Tarazona P 1995 *Phys. Rev.* B **52** 9330
[24] Rosenfeld Y 2000 *Phys. Rev. Lett.* **84** 4272
[25] Kerley G I 1980 *J. Chem. Phys.* **73** 478